

Numerical modeling and design of the acoustic expander for cryogenic refrigeration.

Nathaniel O'Connor^{1*}, Jacob Adams², Matthew Jones¹, and John Brisson²

¹ MIT Lincoln Laboratory, Lexington, MA, USA

² Massachusetts Institute of Technology, Cambridge, MA, USA

*E-mail: nathaniel.oconnor@ll.mit.edu

Abstract. Cryogenic refrigerators can be broadly classified as either continuous flow machines or oscillating flow machines. The acoustic expander is a new hybrid approach that combines the best aspects of these two machines. Globally, the working fluid moves continuously through the recuperative heat exchanger of the cycle while locally the working fluid oscillates in the acoustic expander. This concept has been demonstrated experimentally through the use of reed-valves coupled to an acoustic resonator. This work develops a high-fidelity numerical model that captures non-linear acoustic effects for the future design and optimization of these acoustic expanders. The numerical model solves the fully compressible Navier-stokes equations for various 2D and 3D resonator geometries including both harmonic quarter wave resonators and non-harmonic resonators. The reed valve behavior is simplified using pressure-dependent boundary conditions that can be tuned to represent a variety of reed characteristics. The coupled reed-resonator system spontaneously oscillates at its natural resonance frequency and the numerical model predicts the resonator quality factor and isentropic expansion efficiency. Finally, the numerical model predictions are validated by experimental data. The acoustic expander unlocks new cryogenic cooling paradigms with applications to superconducting magnets and electronics, infrared imaging, quantum sensing, and cryogenic propellant management.

1. Introduction

Cryogenic refrigeration is a critical technology for numerous applications for both scientific research and national security, including infrared imaging, quantum computing, superconducting electronics, and cryogenic propellant storage [1]. Typical cryocoolers can be broadly categorized into either recuperative or regenerative machines, which typically operate with a constant fluid flow or an oscillating fluid flow, respectively. In a recuperative cycle, the working fluid is typically expanded to achieve a cooling effect, either through an orifice or ideally a mechanism which extracts work from the flow, such as a turbine in a reverse-turbo Brayton cycle. Regenerative

DISTRIBUTION STATEMENT A. Approved for public release. Distribution is unlimited.

This material is based upon work supported by the Department of the Air Force under Air Force Contract No. FA8702-15-D-0001. Any opinions, findings, conclusions or recommendations expressed in this material are those of the author(s) and do not necessarily reflect the views of the Department of the Air Force.

© 2024 Massachusetts Institute of Technology.

Delivered to the U.S. Government with Unlimited Rights, as defined in DFARS Part 252.227-7013 or 7014 (Feb 2014). Notwithstanding any copyright notice, U.S. Government rights in this work are defined by DFARS 252.227-7013 or DFARS 252.227-7014 as detailed above. Use of this work other than as specifically authorized by the U.S. Government may violate any copyrights that exist in this work.



Content from this work may be used under the terms of the [Creative Commons Attribution 4.0 licence](https://creativecommons.org/licenses/by/4.0/). Any further distribution of this work must maintain attribution to the author(s) and the title of the work, journal citation and DOI.

cycles alternatively pass a working gas through a regenerator matrix to store heat. Regenerative cycles include the classical Stirling-type cooler, which uses a displacer to achieve a phase shifting between flow and pressure through the regenerator, which acts to shuttle heat. Pulse-tubes have seen significant use for space applications, as by eliminating moving parts at the cold end of the cooler, its reliability is greatly increased. Recuperative cycles can generally achieve high cooling capacities but are difficult to scale down in size, while regenerative cycles struggle to scale up in size. Thus, there exists a gap in expansion devices optimized for mid-scale cooling that can be addressed.

The acoustic expander concept is a novel expansion device that takes advantage of acoustic work dissipation in a recuperative cycle, and eliminates complex moving parts in typical turbine and piston expanders [2]. The acoustic expander relies on a resonator driven by reed valves, which dissipates acoustic work and rejects heat to ambient. In this work, computational fluid dynamics (CFD) numerical models have been developed to capture the behavior of the acoustic expander, including its interaction with the reed valves. Higher fidelity models allow for visualization of the flow patterns within the expander, and can capture non-linear acoustic effects such as streaming. These numerical models will be leveraged to optimize the designs of the acoustic expander to improve its overall expansion efficiency.

2. Numerical Model

The numerical model is implemented in COMSOL Multiphysics version 6.1. Models were developed with both 2D axisymmetric and 3D geometries for the purposes of exploring resonator shapes and reed valve configurations. Several resonators were explored, including a harmonic, $\frac{1}{4}$ wave and a non-harmonic configuration. For the fluid domains, the time dependent, turbulent, compressible, Reynolds-Averaged Navier-Stokes (RANS) continuity, momentum, and energy equations are solved and can be written as,

$$\begin{aligned} \frac{\partial \rho}{\partial t} + \nabla \cdot (\rho \mathbf{u}) &= 0 \\ \rho \frac{\partial \mathbf{u}}{\partial t} + \rho (\mathbf{u} \cdot \nabla) \mathbf{u} &= \nabla \cdot \left[-p \mathbf{I} + (\mu + \mu^T) (\nabla \mathbf{u} + (\nabla \mathbf{u})^T) - \frac{2}{3} (\mu + \mu^T) (\nabla \cdot \mathbf{u}) \mathbf{I} - \frac{2}{3} \rho k \mathbf{I} \right] \\ \rho c_p \frac{\partial T}{\partial t} + \rho c_p \mathbf{u} \cdot \nabla T + \nabla \cdot (-k \nabla T) &= Q \end{aligned}$$

where ρ is density, t is time, \mathbf{u} is the velocity vector, μ is viscosity, μ^T is eddy viscosity, k is turbulent kinetic energy, c_p is specific heat at constant pressure, T is temperature, and Q is heat.

The k- ϵ RANS turbulence model is implemented with wall functions to resolve any high velocity turbulent regions, such as in the jets of gas through the reed valves. Besides the inlet and outlet boundaries for flow through the reed valve, all other boundaries of the fluid domain are no-slip walls such that $\mathbf{u} = 0$. Solid wall domains are also included and simply modelled by the heat diffusion equation. The exterior boundaries of the solid walls have a convective heat flux boundary condition, with a constant convection coefficient of 200 W/(mK) and ambient temperature of 293 K. Importantly, the generalized-alpha time-stepping method is utilized, which reduces the numerical dissipation of higher frequency oscillations, however results in less numerical stability.

Two resonator shapes were explored as shown in Figure 1: A $\frac{1}{4}$ wave resonator and a non-

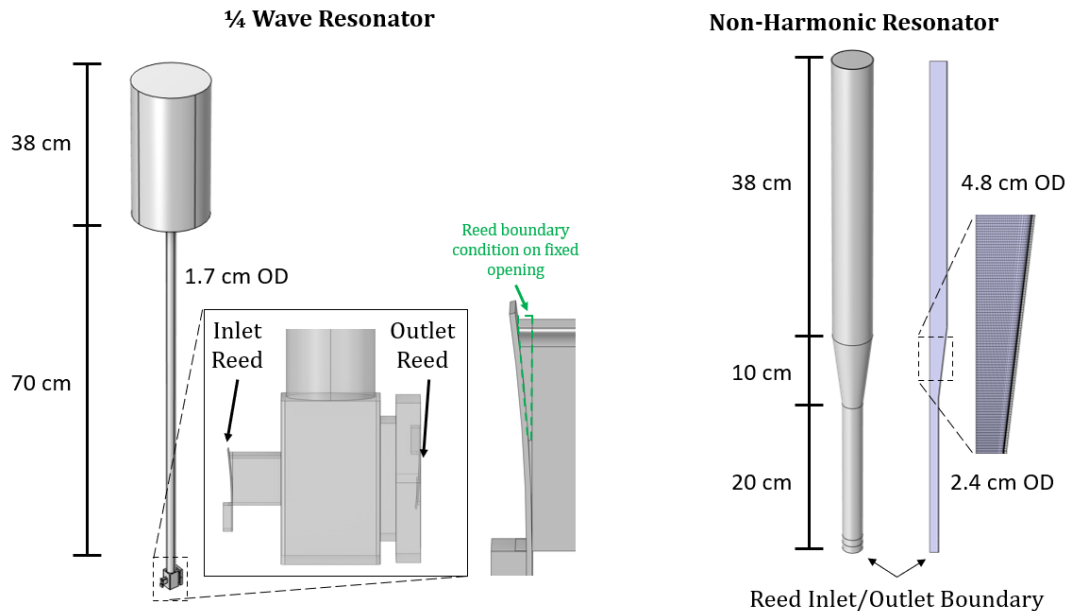


Figure 1. Resonator geometries studied. In the 2D axisymmetric models, the reed inlet and outlet boundary conditions are superimposed at the bottom of the resonator.

harmonic resonator. The $\frac{1}{4}$ wave resonator is a simple straight tube with a volume affixed to one end to approximate an acoustically “open-end” boundary condition. The quarter wave resonator is a harmonic design because the uniform cross-sectional tube is excited by the odd integers of the fundamental frequency. The non-harmonic resonator is a formed by two tubes of different diameters connected with a cone. The variation in cross-sectional dimension means that this resonator is not excited by a harmonic series of frequencies. The suppression of harmonics allows this resonator to operate at higher pressure ratios. Additionally, the non-harmonic resonator has a larger diameter that results in a high-quality factor and the cone acts as a diffuser to limit vortex shedding at the joint between the variable diameter tubes.

2.1 Reed Valve Boundary Conditions

The reed valve behaviour is characterized by a negative flow resistance with increasing pressure, that is to say the flowrate through the reed decreases with increasing pressure differential due to the pressure closing the reed valve. The characteristic flow curve for a single inlet reed is,

$$\dot{V}_{in}(t) = 1.5\sqrt{3} \left[\dot{V}_{max} \left(1 - \frac{\Delta P_{in}(t)}{\Delta P_{max}} \right) \sqrt{\frac{\Delta P_{in}(t)}{\Delta P_{max}}} \right]$$

where \dot{V}_{max} is the maximum flowrate through the reed valve, and ΔP_{max} is the maximum pressure difference that closes the reed valve [3]. $\Delta P_{in}(t)$ is the pressure differential across the inlet reed valve at a given time t , which is calculated based on an assumed constant upstream pressures, P_{high} , minus the oscillating pressure in the resonator. The outlet reed valve follows the same characteristic, except the pressure differential across the outlet reed is the oscillating

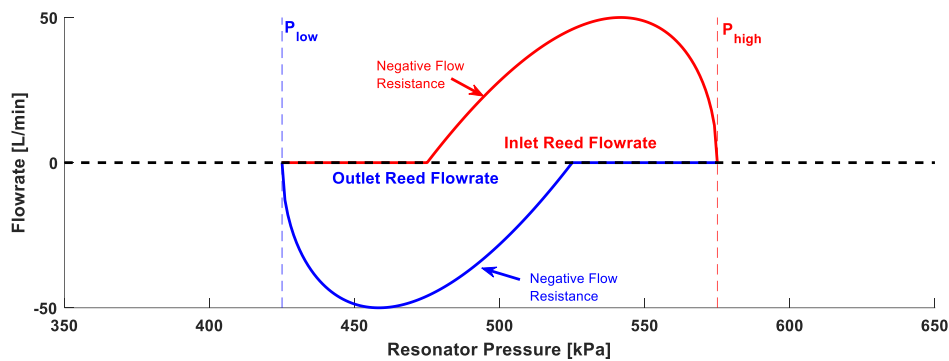


Figure 2. For a fixed reed closing pressure, the overlap of the inlet and outlet flow depends on the imposed upstream and downstream pressure across the resonator.

resonator pressure minus the assumed constant downstream pressure, P_{low} . In the case of the 2D axisymmetric model, the inlet and outlet reed flow conditions are superimposed on one boundary and can be written simply as $\dot{V}(t) = \dot{V}_{in} - \dot{V}_{out}$.

With two reeds interacting with the resonator, the upstream and downstream pressures determine the cadence of flow into and out of the model domain. Utilizing these boundary conditions allows the model oscillate at the natural frequency of the resonator. If both the inlet and outlet reed-valves are biased into their negative resistance regions by the imposed pressure across the expander, then the oscillations will commence. This behavior is illustrated in Figure 2.

3. Model Results

The advantage of the CFD model is the ability to visualize and capture flow behaviors absent in 1D acoustic codes such as DeltaEC. The following section aims to highlight some of the behaviors captured by the CFD model during exploration of various resonator geometries.

3.1 Quarter Wave Resonator

Initial simulations were built around the $\frac{1}{4}$ wave resonator acoustic expander previously demonstrated [2]. Fundamentally, a resonator of this type will be excited to higher harmonics, and this is evidently observed in the experimental data as a square wave response in pressure at the bottom of the resonator. Figure 3 shows the start-up and pseudo-steady state resonator response in the numerical model driven by the reed boundary conditions with a maximum flowrate of 30 L/min and maximum differential pressure of 130 kPa. The resonator tube has a length of 70 cm and a diameter of 1.7 cm. The resonator upstream and downstream pressure is set to 575 kPa and 350 kPa, respectively. Initially the resonator is at the mean pressure of 525 kPa, and an initial perturbation of 10 kPa is introduced. The system naturally begins to oscillate at a frequency of 113 Hz and the pressure oscillations build. The resulting pressure waveform is not purely sinusoidal, there are higher harmonics of the fundamental present. However, some of the higher harmonics are numerically dissipated and limited by the resolution of the mesh. The isentropic expansion efficiency of the expander can be evaluated through the temperature of the gas exiting

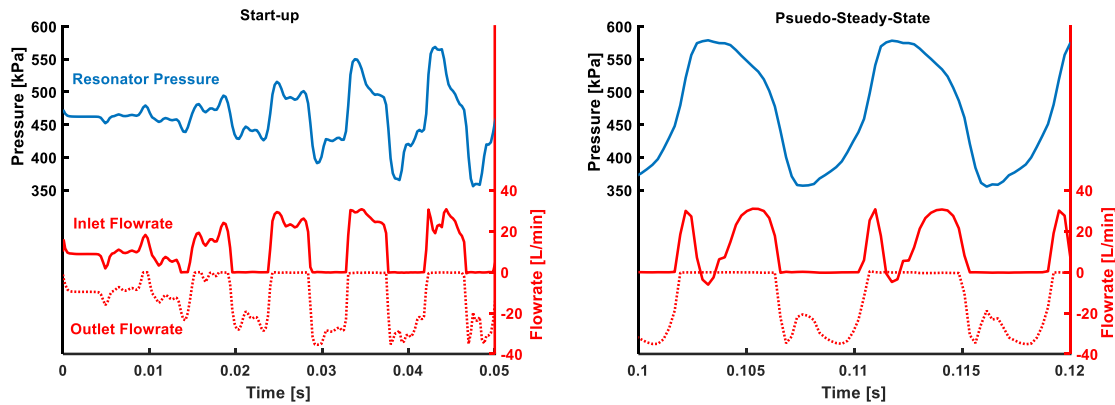


Figure 3. Pressure and reed flowrates for the ¼ wave resonator. The response includes higher harmonics, however high frequencies are dissipated numerically.

the outlet reed. The ideal isentropic outlet temperature based on the imposed high and low pressures is compared against the mass flow weighted average of the outflowing gas temperature.

$$T_{out}^W = \frac{\sum_{i=1}^n T_{out}(t_i) \dot{m}_{out}(t_i)}{\sum_{i=1}^n \dot{m}_{out}(t_i)}, T_{out}^{isentropic} = T_{in} \left(\frac{P_{out}}{P_{in}} \right)^{\frac{\gamma-1}{\gamma}}, \eta_{isentropic} = \frac{T_{in} - T_{out}^W}{T_{in} - T_{out}^{isentropic}}$$

The model calculated efficiency for this acoustic expander is 55%, comparable with the previously reported experimental data [2].

3.2 Non-Harmonic Resonator

The non-harmonic resonator design features a conical section that results in an area change. This resonator is excited by its fundamental frequency, and does not have integer harmonics, thus the resulting pressure oscillations are sinusoidal. This model was built in a 2D axisymmetric geometry, so the reed geometry is neglected. From an initial 10 kPa disturbance, the pressure oscillations in the resonator begin to build. A higher pressure ratio of 2.33 is imposed, with 700

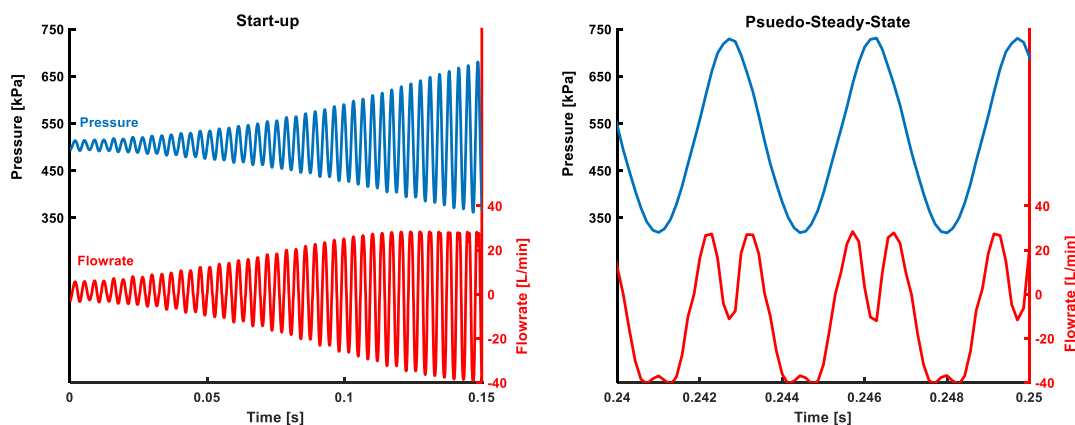


Figure 4. Start-up of non-harmonic resonator with imposed pressure ratio of 2.33. The large differential pressure necessitates reed valves with a large maximum closing pressure.

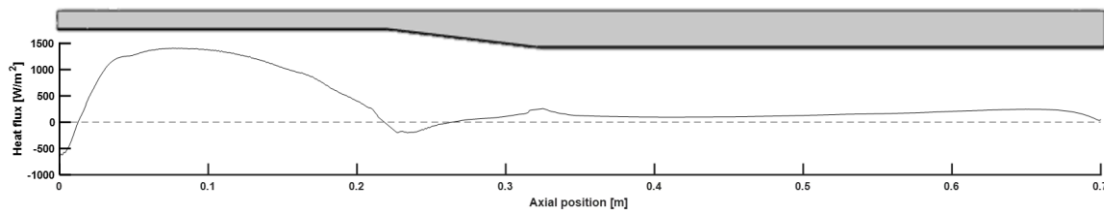


Figure 5. Time-averaged heat flux along the non-harmonic resonator.

kPa on the high pressure side and 300 kPa on the low pressure side. A reed boundary condition is implemented with a maximum mass flowrate of 4 g/s and maximum differential pressure of 200 kPa. Figure 4 shows the start-up of the sinusoidal pressure oscillations in the resonator leading to steady operation after a 25 kPa initial disturbance.

Including solid domains in the model allows for the capturing of heat shuttling effects present due to the phase shift between flow and pressure in the resonator. While the resonator is observed to heat significantly during experiments, it is apparent from the CFD model that there is a heat shuttling effect that pumps heat towards the cold end of the resonator. Figure 5 shows the time averaged interior wall heat flux. It can be seen that there is significant heating in the high velocity region of the resonator, where viscous dissipation is maximized. The proximity of the heat dissipation to the cold end of the expander is another potential source of inefficiency, and thus it is desirable to design a resonator that dissipates the acoustic work as far from the cold end as possible. This can be achieved with mesh or screens located within the far end of the resonator.

With the development of representative CFD models of the acoustic expander, focus can now be shifted towards design and optimization of these devices. The models can be used to optimize the geometry and shape of the resonator to improve efficiency and mitigate effects such as acoustic streaming. The models can also aid in the expander design tailored to specific applications in cryogenics. Further model development areas include studying interaction with the upstream and downstream flow plenums with the resonator, and optimization of reed valve performance.

5. Conclusions

A CFD model has been developed to simulate the performance of acoustic expanders. Pressure dependent boundary conditions representative of the reed valves allow the model to capture the start-up behavior and evaluate the performance of the expander, which is not possible with existing 1D thermoacoustic codes. The model is shown to capture the behavior of the acoustic expander and is validated against experimental data. These models can be applied to further optimize the performance of the expander, and design towards specific applications of cryogenic refrigeration.

References

- [1] *Active cryocooling needs for NASA space instruments and future technology development.* Weibo Chen, Michael DiPirro, Ian McKinley, Chulhee Cho, Howard Tseng. 2024, Cryogenics, Vol. 141. 103877.
- [2] *Acoustic Expanders for Use in Recuperative Cryocoolers.* Jacob L. Adams, J. G. Brisson. 2024. IOP Conf. Ser.: Mater. Sci. Eng. Vol. 1301. 012134.
- [3] N. Fletcher and T. Rossing (1991), "The Physics of Musical Instruments." Springer